TWO PHASE EQUILIBRIUM DISTRIBUTION IN THREE- DIMENSIONAL POROUS MICROSTRUCTURES

P.C. PHILIPPI[◇], F.S. MAGNANI[*], A. D. BUENO
Mechanical Engineering Department, Federal University of Santa Catarina, Cx. P. 476
88040-900 Florianópolis SC, Brazil

ABSTRACT

This work presents a methodology for determining the interface between wetting and non-wetting phases inside a three-dimensional porous space, at a given equilibrium state. The work is limited to the study of mechanical equilibrium. The method is based on a three dimensional extension of the opening method from image analysis presented in [1] and applied on three-dimensional stochastically reconstructed porous microstructures of reservoir rocks. The great advantage of the presently proposed methodology with respect to percolation networks conception is that simplifying assumptions regarding the geometry of the porous space are avoided. In fact, invasion of wetting fluid in imbibition and wetting fluid retention in the later stages of drainage occur spatially through a complex structure of corners and intrinsic irregularities of pore surfaces that are very difficult to model using percolation networks of sites and bonds. Simulation results were compared with experimental data related to mercury intrusion and water-oil capillary curves were simulated for several distinct cases.

Keywords: two-phase mechanical equilibrium, three-dimensional porous structures.

Paulo C. Philippi is Professor at Federal University of Santa Catarina where he heads the Porous Media and Thermophysical Properties Laboratory (LMPT). He specializes in image analysis and processing, single and multiphase flow in porous media and lattice gas automata (LGA) methods

Fabio Santana Magnani is Associate Professor at Federal University of Pernambuco. He specializes in image analysis and processing and multiphase flow in porous media.

André Duarte Bueno has BS and MSc degrees in Civil Engineering. He presently makes his Doctoral studies in Porous Media and Thermophysical Properties Laboratory (LMPT) which includes equilibrium phase distribution and prediction of relative permeability in porous media..

◇ Corresponding author
* Presently at Mechanical Engineering Department of Federal University of Pernambuco 50740-530, Recife PE, Brasil.

1. INTRODUCTION

The problem of predicting macroscopic transport properties from the underlying microscopic structure and pore-scale physics has been the subject of extensive investigation in recent years.

Conceived as a dynamical problem, two-phase fluid invasion into a porous structure is complicated due to the difficulty in predicting the location of the interface between the two fluids as it is the site of dynamical unstability sources, considering the competition between inertial forces, surface tension and viscous transfer of momentum. In the present work, two-phase fluid invasion is supposed to proceed following a sequence of quasi-static processes between equilibrium states. The dynamic invasion problem is, thus, strongly simplified and reduced to the determination of the interface between the two fluids by using the well-known Young-Laplace equation. In fact, Young-Laplace equation predicts a *constant curvature* for an interface in mechanical equilibrium. The location of the interface can, thus, be regarded as a *geometrical problem*.

The purpose of this work is to present a methodology for determining this interface, considering two non-miscible phases inside a three-dimensional porous space, at a given equilibrium state. The work is limited to the study of mechanical equilibrium: mass transfer between the phases is not considered. The method is based on a three dimensional extension of the opening method from image analysis. At the authors' knowledge, this idea was firstly used in the study of water vapour sorption in two-dimensional porous sections by Quenard and Bentz [2], although Delfiner *et al.* [3] were the first to propose the use of opening methods, in the simulation of mercury intrusion. Recently, Yao *et al* [4] have used this method for study mercury intrusion into three-dimensional porous structures reconstructed from the data obtained from Vosges sandstone.

The methodology used here was presented at Magnani *et al* [1]. This paper describes some main results related to mercury intrusion simulation and to water-oil capillary equilibrium curves of main interest for petroleum industry.

The great advantage of the proposed methodology with respect to percolation networks conception is that simplifying assumptions regarding the geometry of the porous space are avoided. In fact, invasion of wetting fluid in imbibition and wetting fluid retention in the later stages of drainage occur spatially through a complex structure of corners and intrinsic irregularities of pore surfaces that are very difficult to model using percolation networks of sites and bonds.

2. MATHEMATICAL MODELS

2.1 Mathematical model for the three-dimensional representation of the porous structure

Figure 1 shows two digital segmented image, in (a) a Berea500 sandstone and (b) a Brazilian sandstone, showing the porous phase in black and the solid phase in white. Image was obtained from a thin plate of Berea sandstone and Brazilian sandstone, after scanning with an optical microscope, pre-processing and, lastly, segmentation by the method of maximal interclass variance (details can be found in a companion paper [5]).

Three-dimensional reconstruction is based on the assumption that the genesis of porous structure follows a stationary stochastic process, presenting the same statistical moments measured at the 2D representation.

Several methods exist to generate discrete random fields. Adler *et al.* [6] and Fernandes [7] generated isotropic media by a simplified version of an algorithm presented by Quiblier [8] for general 3-D porous media based on truncated gaussian method. This algorithm was itself an extension of a 2-D scheme devised by Joshi [9]

In this paper, is used the truncated gaussian method by applying Fourier transform, as proposed by Liang *et al* [10]. The method consists in generating a random function $Z(\mathbf{x})$ that is equal to zero in the solid phase and to one in the pore phase and which preserves porosity and auto-

correlation function. The analysis is restricted to homogeneous media, where the statistical characteristics are assumed to be independent of position **x** in space. Due to homogeneity, porosity is a constant and $R_Z(\mathbf{u})$ depends only upon the displacement vector **u**. Moreover, when the porous medium is isotropic, R_Z is a function only of $u=|\mathbf{u}|$.

Given a positive-definite function $R_Y(u)$, it is possible to find a stochastic process $Y(\mathbf{x})$ having $R_Y(u)$ as its normalized auto-covariance function. By definition of Fourier transform and the Wiener-Khinchin theorem, the Fourier transform of the correlation function of a field is also its power spectrum. Therefore, if the correlation function of an arbitrary field is known, one can use Fourier transform to generate this field $Y(\mathbf{x})$ with the same auto-covariance function (Pardo-Igúzquiza and Chica-Olmo [11]. The difference between this method and previous ones is that $Y(\mathbf{x})$ is directly generated from its auto-correlation function $C(\mathbf{u})$, and does not need the linear filter transform $X(\mathbf{x})\rightarrow Y(\mathbf{x})$. In addition, when compared with Adler's method [6], Liang *et al* method [10] reduces the resident memory requirements, because the independent gaussian field data $X(\mathbf{x})$ are not needed.

Three-dimensional reconstruction needs information about porosity ε and auto-correlation function $C(\mathbf{u})$. Considering isotropic sections, auto-correlation function is, usually, calculated along a given direction by displacing the binary representation over itself in the x direction (or y), using multiples of the pixel dimension and measuring the void fraction related to the intersection, i.e., the frequency of outcomes corresponding to two superposed black pixels (Adler [6] and Philippi *et al.* [12]).

Due to the finite size of this *discrete* binary representation with respect to pixel dimension, the above described procedure produces, generally, fluctuations on auto-correlation function. Since auto-correlation function C(u) is related to the *probability* of finding two points separated by u and belonging to the same phase, it is advantageous to calculate $C(\mathbf{u})$ as a function of the two-dimensional vector $\mathbf{u}=(x, y)$ and, then, to take its mean value around a circle with radius $u=|\mathbf{u}|$. This last procedure produces more reliable C(u) values since it increases the number of realizations needed to calculate this probability.

The utilization of presently well known and largely diffused fast algorithms, makes Fourier transform a very suitable tool to calculate $C(\mathbf{u})$, as a function of the displacement vector $\mathbf{u}=(x, y)$. Using Wiener-Khinchin theorem, normalized auto-covariance function $R_Z(\mathbf{u})$ was measured by calculating the power spectrum of the phase function $Z(\mathbf{x})$, i.e.,

$$R_Z(\mathbf{u}) = \Im^{-1}\left|\hat{Z}(\mathbf{p})\right|^2, \qquad (1)$$

where $\hat{Z}(\mathbf{p})$ means the direct Fourier transform of $Z(\mathbf{u})$ and $\Im^{-1}$ is used to indicate the corresponding inverse operation. Taking the mean value of R_z for the several **u** with the same norm produces $R_Z(u)$, used in the present work to three-dimensional geometrical reconstruction of the porous structure.

Figure 2 shows a three dimensional view of the reconstructed microstructure for a given realization.

2.2 Mathematical model for the fluid invasion problem

Capillary invasion is a difficult dynamical problem where the interface between fluids is subjected to wall surface potentials, inertial forces, interfacial tension and viscous transfer of momentum. Present model uses the simplifying assumption that equilibrium phase configurations are attained, inside the porous structure, following a quasi-static process.

The geometrical problem was presented in Magnani *et al* [1]. Model's main features are presented bellow. Consider a system, U, composed by a rigid porous sample, $M \subset U$ (Figure 3). It is supposed that both M and S (the solid phase) remain invariant during any process. The constancy of M and S assures, respectively, that the porous body is macroscopically and microscopically rigid.

Additionally, it is supposed that the two fluids are non-miscible and the present work is only concerned with quasi-static processes.

Consider an invasion process where a fluid B displaces a fluid A initialy inside the porous space. Let this process be considered as a sequence [i, i=0,1,..,p] of elementary steps between equilibrium states. For each step i, B^i is the geometric region occupied by fluid B and, for step 0, B^o is such that $B^o \cap P = \phi$, i.e., the invader fluid is outside the porous body at the beginning of the process. For each step i, B^i is a connected geometrical region, while A^i is the union of several geometrical regions which became disconnected during the invasion process.

In fact,

$$A^i = A_o^i + \bigcup_{k=1}^{n(i)} A_k^i , \tag{2}$$

where, in step i, A_o^i is the geometrical partition of A which remains connected to the free region L during the invasion process and A_k^i , k=1,...,n(i), is one of the n(i) regions in F which became disconnect from L due to trapping by fluid B.

The trapped domain Y at step i is formally defined as:

$$Y^i = A^i - A_o^i \quad 1 \le i \le p, \tag{3}$$

At step i of invasion, let E_x^i be a ball of radius r^i, centered at x, for a given point x belonging to region F, i. e., the union of the porous region, P and the free region, L. Radius r^i is determined from the well known Young-Laplace equation, which establishes the equilibrium condition at the interface between fluids A and B,

$$r^i = \left| \frac{(d-1)\sigma_{AB}}{P_{A_o^i} - P_{B^i}} \right| , \tag{4}$$

where d is the Euclidian dimension of the space, σ_{AB} is the interfacial tension between fluids A and B, $P_{A_o^i}$ is the pressure at the domain of fluid A which is connected to the free region L, and P_{B^i} is the pressure of fluid B, at step i.

For points x that are closer than r^i from the boundary of F, the ball E_x^i will intercept this boundary. For this reason a new ball E_x^{*i} is defined such that,

$$E_x^{*i} = \begin{cases} E_x^i & \text{if } d_x \ge r^i \\ \phi & \text{if } d_x < r^i \end{cases} \tag{5}$$

where d_x is the smallest of the distances between point x and the boundary of F.

An opening region H is defined such that at step i,

$$H^i = \bigcup_x E_x^{*i} \quad x \in F \tag{6}$$

H^i is a region whose interface has one of its two curvature radius constant and given by r^i. As it is the union of spherical balls enclosed in F, this interface makes a contact angle of 0^o with the solid boundaries, defined with respect to the wetting phase.

For simulation purposes, the free region L is constructed with a boundary having a finite curvature radius. In this manner, a new opening region is defined, as,

$$G^i = L \cup H^i \tag{7}$$

It is important to define a complementary region of G^i, to find the phase distribution in the porous phase at step i, as

$$\underline{G^i} = F - G^i \tag{8}$$

Let J and Q be any two regions of F and let K(J,Q) be a union operator defined as the union of the connected components J_j of J with a non-null intersection with Q,

$$K(J,Q) = \bigcup_{k=1}^{n(J)} \begin{cases} J_j & \text{if } J_j \cap Q \neq \varnothing \\ \varnothing & \text{if } J_j \cap Q = \varnothing \end{cases} \tag{9}$$

Evidently,

$$K (K(J,Q),Q) = K(J,Q) \quad (10)$$

For a set $\aleph$, defining $a\aleph$ to be $\aleph$ when a=1 and to be the null set $\varnothing$ when a=0, the geometrical region occupied by fluid B can be determined using the following equation:

$$B^i = \Omega^i - u_A Y^i, \quad (11)$$

where:

$$\Omega^i = K\{ [(w_B) \underline{G}^i \cup K(G^i, B^0)] , B^0 \}, \quad (12)$$

and w_B is a wetting factor for fluid B (w_B=1, when fluid B is the wetting fluid and w_B=0 otherwise), u_A is a compressibility factor for fluid A (u_A=0 for fluids which are ideally compressible and u_A=1, for fluids which are ideally incompressible). When fluid A is incompressible, domain B at step i is, thus, dependent, on the trapped domain Y^i, which is not known at this step. In present work, domain Y^i is approximated by the geometrical region that is trapped at step i-1, $Y^i \approx Y^{i-1} = A^{i-1} - A_o^{i-1}$. The degree of approximation will be, therefore, dependent on the step extent between two consecutive equilibrium states. In a three-dimensional discrete representation of the porous microstructure, this means, by Eq.-(4), that reliability of present simulation model, will be dependent on voxel linear dimension (volume element).

3. COMPUTATIONAL ASPECTS

Computational procedure starts from a three-dimensional phase function Z(**r**) whose domain U is a cube, representing the system to be analyzed, including the porous material and the chambers where the wetting and non-wetting fluid are to be placed, for simulation purposes. Z(**r**)=0 if $\mathbf{r} \in S \cup T$ and Z(**r**)=1 if $\mathbf{r} \in F$. In the first step, the distance d_x, defined in Eq. (5) is determined for each $r \in F$. Distance d_x is the smallest of the distances from point $\mathbf{r} \in F$ to the boundary between region F and solid phases and will be, in the following text, called *background distance (BD)*.

For a three–dimensional system, **r** is a discrete variable and each **r** is associated to a given three dimensional cell in space. Present paper deals with a chanfer metric, considering the distance between the centers of two adjacent cells as 3, the distance between two adjacent cells with a common edge as 4 and 5 when they have a common corner.

To find the distance of each cell to the background (BD), a corner is chosen as the starting point, and the cells of the first plane, z=0, are labeled. In the next z planes, distance is calculated using a 3-4-5 spatial chanfer mask. The procedure is sequential, following the 0-x, 0-y and 0-z directions. Cells in the solid phase are labeled with 0, and the first cells in phase F, with a face, an edge or a corner adjacent to the solid phase are labeled with 3, 4 or 5, respectively. Chanfer distances can be stored in a ordinary computer as integers, using a 2 bytes address, instead of 4 bytes, necessary for real variables (in 32 bits platform). Further details can be found in Magnani *et al* [1].

Matrix BD(x, y, z) is important to find the several geometrical regions defined in Section 2. In this way, the opening region H^i, defined in Eq. (6), is obtained at step i, by placing a ball of radius r^i centered at each cell with a BD, satisfying

$$r^i < BD \leq r^i + 1 \quad (13)$$

and by considering all cells with $BD \geq r^i + 1$ as belonging to H^i. In fact, balls with radius r^i centered on cells with BD$\leq r^i$ intercept the boundary of phase F and cells with $BD \geq r^i + 1$ are always surrounded by cells with $BD > r^i$. Region G^i as its complement $\underline{G}^i$ can be then determined using Eqs. (7) and (8).

In the present paper, determination of K(J,Q) was improved with respect to older version exposed in Magnani *et al* [1], by adding a three-dimensional labeling algorithm, reducing total processing time to about 9%.

4. RESULTS

The above procedure was used to simulate mercury intrusion and wetting / non-wetting fluid invasion into a three-dimensional reconstructed representations of Berea500 sandstone and of Brazilian sandstone P30.5K642 found in a Petrobras petroleum reservoir (images were furnished by CENPES/Petrobras) .

4.1 Three dimensional geometrical reconstruction

Figure 4 shows a comparison for the cumulative porous volume fraction measured as the mean taken from 10 binary images and the mean values obtained from the 2D cross sections of the reconstructed microstructure of P30.5K642. Reconstruction was performed by generating three-dimensional cubes with N=200 voxel as linear size. This linear size was verified to be large enough to ensure statistical homogeneity, giving three-dimensional representations with statistical averages independent of the random seed used in the reconstruction. Curves of the porous volume fraction were obtained by measuring the cumulative area fraction on all 2D serial cross sections sliced from the reconstructed three dimensional representation and by taking the average between these sections, for a given ball radius. Opening operation from image analysis was used in this computation step (Chassery and Montanvert [13]). Factor n is a sampling factor taken over $R_Z(u)$ data: sampling factor n means that the only points considered for $R_Z(u)$ data were the ones separated by n-1 pixels.

Results show that, when sampling factor n (SFn) is reduced, three-dimensional reconstruction gives a systematic deviation with a larger amount of small size pores when compared to the original binary image and that this amount is underestimated, when sampling factor increases. The better agreement was obtained for n=2. This systematic deviation is possible to be attributed to the reconstruction method itself, which appears to fail when trying to preserve the size distribution of the smaller features found in the original 2-D binary image. In fact, it must be remembered that present reconstruction method is based: i) on the hypothesis that the target original two-dimensional representation is a realization of a stochastic process which is considered to be ergodic and stationary and ii) on the hypothesis that this process is gaussian and can be, inherently, described by its only two first moments.

4.2 Mercury intrusion

Prediction of mercury intrusion based on image analysis methods carried on petrographic thin plates has the following main limitation: acquired digital images must be large enough to ensure statistical homogeneity, implying in low resolution (or, equivalently, in a large ratio μm/pixel).

Attainable resolution is, typically, about 2μm/pixel at 50X magnification. Higher resolutions can be attained with higher magnification and working with digital image assemblages. However, color uniformity is difficult to achieve and computer resident memory limitation imposes an upper limit to this procedure.

In this way, ordinary simulation is limited to about 3atm, which is considerably lower than the 2000 atm nominal limit of current mercury intruders.

Nevertheless, in despite of this limitation, mercury intrusion simulation based on petrographic thin plates, can be useful in the understanding of the *early* mercury intrusion stages, which is mainly conditioned by reservoir rock macroporosity. In addition, considering that intrinsic permeability of reservoir rocks is frequently related to its macroporosity, mercury intrusion simulation can furnish valuable information such as percolation thresholding diameter and/or other input data in the estimation of intrinsic permeability.

In present paper, mercury intrusion was simulated, on reconstructed three-dimensional representation by using different simulation methods, named nF, where mercury intrusion is supposed to proceed through n external surfaces of the 3D representation. In addition, simulation was, also, performed supposing intrusion to proceed from an internal chamber. This method, named *internal intrusion* (see Figure 5), has the advantage of decreasing surface/volume ratio, reducing surface effects of the three-dimensional representation.

Figure 6 shows a three-dimensional representation of the sequential evolution of mercury intrusion, proceeding from a single external surface, method 1F, for different pressure steps.

Mercury intrusion was simulated in three-dimensional reconstructed porous structures of several reservoir sandstones. Measured intrusion pressures were converted to ball radius using Young-Laplace equation, corrected by the cosine of the contact angle. Experimental values proceed from mercury intrusion experiments performed in CENPES/Petrobras.

4.3 Effects of simulation method and of the 3D representation linear size

Figure 7 shows a sequence of simulation results when 3D representation linear size N is increased from 50 to 300. Different curves refer to different intrusion methods: 1F, 2F, 4F, 6F and internal intrusion. Experimental values are related to Berea500 sandstone and reconstruction was performed with a sampling factor n=4, starting from a single petrographic thin plate, where source digital image was taken with a resolution of 2.6 μm/pixel. It is clearly seen that for small linear size, intrusion results are very sensitive to the particular simulation method used. Percolation threshold is retarded when intrusion surface is reduced, as expected. This influence is reduced as linear size N increases. When compared to experimental results, the best simulation corresponds to method 6F, where mercury intrusion is supposed to happen through all the 6 external sample surfaces, best corresponding to *real* intrusion experiment. As asserted above, internal intrusion reduces surface/volume ratio due to finite volume effects and would best correspond to a hypothetical intrusion experiment performed into very large samples.

Figure 8 shows the influence of sampling factor 'n' on simulation results for P30.5K642 Brazilian sandstone, see Figure 1(b). Simulation was performed using a 200^3 voxel, reconstructed representation considering 6F mercury intrusion simulation method. As shown in Section 4.1 sampling factor n=2 gave the best agreement between measured and simulated pore size distribution. Present results authenticate this previous result and validate present methodology for predicting the early stages of mercury intrusion. As asserted above, late stages of mercury intrusion are related to very small porous cavities and spatial resolution obtained in acquiring digital images from petrographic thin plates is considerably beyond the minimal resolution that is necessary to simulate late mercury intrusion stages.

4.4 Simulation of wetting/non-wetting quasi-static displacement

Water-oil capillary displacement is an important physical process in petroleum engineering. Laboratory tests are, usually, performed in centrifuges furnishing water-oil capillary curves, which are important source of information for the prediction of petroleum recovery performance.

Present section deals with immiscible quasi-static displacement of a non-wetting fluid A, initially filling the whole porous space, by a wetting fluid B. Process starts from an equilibrium state where capillary pressure $P_A - P_B$ is supposed to be high enough to prevent wetting fluid invasion. In this way, when capillary pressure is decreased, wetting fluid invasion proceeds through the corners and smaller pores of the porous structure, producing blockage of the non-wetting fluid. These effects are very important in wetting fluid invasion and entirely justified from a physical point of view. They cannot be predicted by, e.g., percolation networks, although several attempts have been made in the last few years for taking account of edge invasion, by the use of networks with square cross sections bonds, connecting cubic sites (Ioannidis and Chatzis14). In fact, the extreme irregularity of the porous surface produces a very complex network of three-dimensional bonds for wetting fluid invasion, which is very difficult to model by using percolation networks. In

the present conception, corner invasion is an intrinsic consequence of the method used to predict the geometrical regions occupied by the wetting and non-wetting phases, inside the pore space.

Figure 9 shows a 3D visualization of simulation results for wetting fluid invasion.

Figure 10 shows simulation results for wetting fluid B invasion into Berea500, 80^3 and 330^3 reconstructed representations using sampling factor n=4, initially filled with an ideally compressible non-wetting fluid A. Wetting and non-wetting phases will become connected for capillary pressures corresponding to ball radius between, about, 10 and 40 μm. In present case, trapping of non-wetting fluid has no consequence as it is considered as ideally compressible.

Figure 11 shows similar results for wetting fluid B invasion into 330^3 Berea500, reconstructed representation, initially filled with an ideally uncompressible non-wetting fluid A. Wetting and non-wetting phases will become connected for capillary pressures corresponding to ball radius between, about, 10 and 20 μm. In present case, due to uncompressibility, non-wetting fluid which is blocked during invasion will remain trapped during the whole invasion process. In fact, in present case, near 45% of non-wetting fluid remains trapped in the porous space. Although experimental results were not disposable for this sample case, trapped volume fraction of non-wetting fluid is expected to be larger than the one obtained in present simulation. In fact, proceeding through the corners and smaller pores of the porous structure, wetting fluid invasion is expected to be very sensible to porous structure details: in present case, simulation was performed inside a porous space representation reconstructed with sampling factor n=4, where the fine porous structure was lost in the reconstruction process.

A more interesting sample case, is represented by Berea sandstone simulation, when 3D representation is reconstructed with n=1 (Figure 12). In this case, although porous structure fine details were overestimated in the reconstruction process, results give a lager volume fraction of trapped non-wetting fluid, which amounts to 55%.

Figure 13 shows simulation results, obtained when the invader fluid is non-wetting. Pressures P_A and P_B are initially the same, and invasion proceeds by increasing P_B with respect to P_A. In this way process proceeds in the negative direction of x-axis in Figure 11, beginning with the larger ball radius it is possible to place inside the porous space and finishing with a ball radius equal to 1 voxel. Points corresponding to ball radius r=0, were not directly obtained in the simulation: one considers that connected portion of wetting phase is zero at the end of drainage and that the volume amount of blocked wetting fluid remains the same after the last simulation point. Although these assumptions are somewhat arbitrary, it is very difficult, from a computational point of view, to increase details in the last end of drainage, as each additional simulation point require to *double* resident memory requirements in the simulation process. Results show that about 35% of wetting fluid volume remain trapped at the end of drainage. In this case, it is expected that the trapped volume of wetting fluid is almost *insensible* to the details of porous fine structure. This was verified in some few cases, by resampling the 3D reconstructed representation: trapped volume remained the same in all performed drainage simulations.

5. CONCLUSIONS

In present paper, a methodology was presented for studying two-phase equilibrium inside a porous medium, based on Young-Laplace's equation that predicts a constant curvature for the interface between two-phases in mechanical equilibrium. The great advantage of the presently proposed methodology with respect to percolation networks conception is that simplifying assumptions regarding the geometry of the porous space are avoided. The method is applied on three-dimensional reconstructed porous structures.

Simulation of mercury intrusion and water-oil capillary curves are presented and compared with experimental data. Corner invasion and retention of wetting fluid during the later stages of drainage are, apparently, adequately modeled, especially when compared with percolation networks models. Considering the limitations of the methodology, results apparently confirm its adequacy as a valuable tool for simulating two-phase equilibrium in porous media.

ACKNOWLEDGEMENTS

The authors would like to acknowledge CENPES/PETROBRAS (Centro de Pesquisas e Desenvolvimento Leopoldo A. Miguez de Mello) for providing the images and experimental data for Berea and Brazilian sandstones and financial support of CNPq (Conselho Nacional de Desenvolvimento Científico e Tecnológico), PADCT (Programa de Apoio ao Desenvolvimnto Científico e Tecnológico), RHAE (Programa de Formação de Recursos Humanos em Areas Estratégicas) and FINEP (Financiadora de Estudos e Projetos).

6. REFERENCES

[1] Magnani F.S., Philippi P.C., Liang Z.R. and Fernandes C.P., 2000, *Modelling two-phase equilibrium in three-dimensional porous microstructures,* **Int. J. Multiphase Flow., 26** (1), 99-123.

[2] Quenard D. A. and Bentz D.P., 1992, *Capillary condensation, hysteresis and image analysis,* **Proceedings of Drying' 92 Symposium**, 253-262.

[3] Delfiner P., Étienne J., and Fonck J.M., 1972, *Application de l'Analyseur de Textures a l'Étude Morphologique des Réseaux Poreux em Lames Minces,* **Revue de l'Institut Français du Pétrole XXVII** (4), 535-558.

[4] Yao J., Thovert J.F., Adler P.M., Tsakiroglou C.D., Burganos V.N., Payatakes A.C., Moulu J.C., and Kalaydjian F., 1997, *Characterisation, reconstruction and transport properties of Vosges sandstones.*, **Revue de l'Institut Français du Pétrole 52** (1), 03-21.

[5] Damiani M.C., Fernandes C.P., Bueno A.D., Santos L.O. E., Cunha Neto J.A.B., and Philippi P.C., *Predicting Physical Properties of Reservoir Rocks from the Microstructural Analysis of Petrographic Thin Sections.* **Submitted to Produccion 2000 / Aplicaciones de la ciencia en la ingeniería de petróleo**, May 08-12 /2000, Foz de Iguaçu.

[6] Adler P.M., 1992, *Porous Media: Geometry and Transports.* **Butterworth - Heinemann**, New York.

[7] Fernandes C. P., 1994, *Caracterização Morfotopológica de Espaços Porosos: Reconstituição Multi-Escala e Simulação de Processos de Invasão de Fluidos Não-Molhantes.*, **Doctoral Thesis**, Mechanical Engineering Department, Federal University of Santa Catarina, Florianópolis.

[8] Quiblier J.A., 1984, *A new three-dimensional modelling technique for studying porous media.* **Journal of Colloid and Interface Science**, 98, 84-102.

[9] Joshi M.Y., 1974 *A Class of Stochastic Models for Porous Media.* **Ph. D. thesis**, University of Kansas, Lawrence, U.S.A.

[10] Liang Z. R., Fernandes C.P., Magnani F.S., Philippi P.C., 1998, *A reconstruction technique for 3-D porous media using image analysis and Fourier transforms.* **J. Petroleum Science and Engineering** (in press).

[11] Pardo-Igúzquiza E. and Chica-Olmo M., 1993, *The Fourier Integral Method: An Efficient Spectral Method for Simulation of Random Fields.*, **Mathematical Geology, 25**, 177-217.

[12] Philippi P.C., Yunes P.R., Fernandes C.P., and Magnani F.S., 1994, *The Microstructure of porous building materials: study of a Cement and Lime Mortar.* **Transport in Porous Media,** 14, 219-245.

[13] Chassery J.M. and Montanvert A., 1991, *Géométrie Discrete en Analyse d' Images,* Hermes, Paris.

[14] Ioannids M.A. and Chatzis J., 1993, *The effect of spatial correlations on the accessibility characteristics of three-dimensional cubic networks as related to drainage displacements in porous media.* **Water Res. Research,** 29, 1777-1785.

7. FIGURES

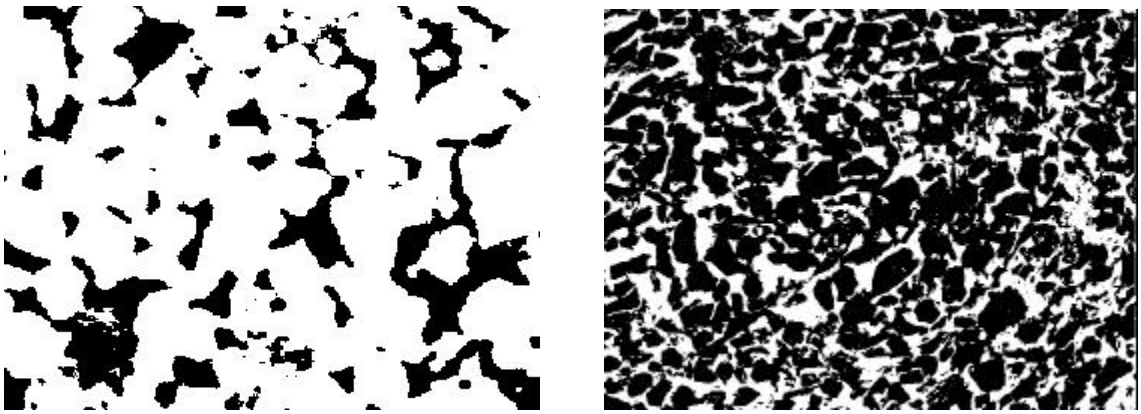

(a) (b)

Figure 1: (a) Segmented image of a 2D section of Berea500 sandstone (magnification 50X)

(b) Segmented image of a 2D section of Brazilian sandstone (P30.5K642)

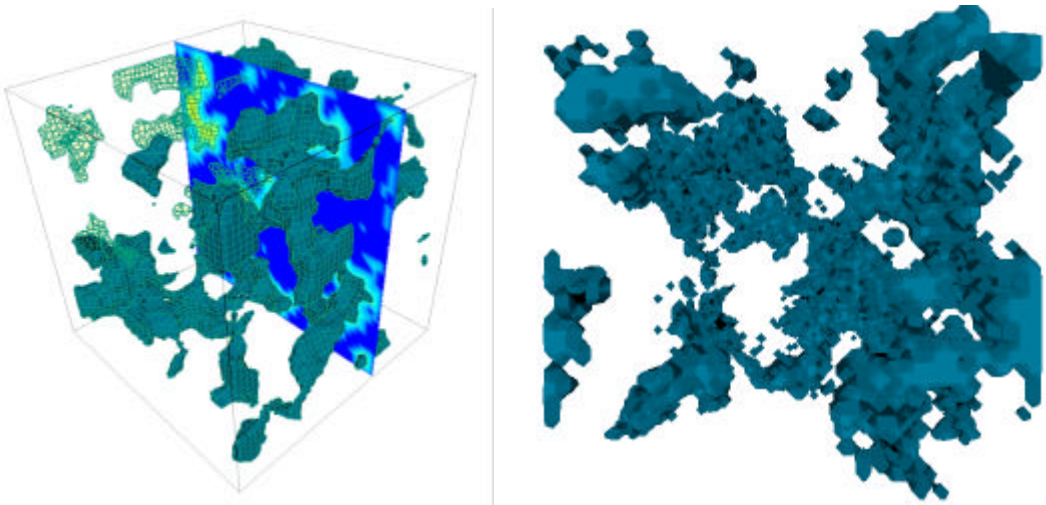

(a) (b)

Figure 2: Three-dimensional representation of (a) Berea500 sandstone (b) Brazilian sandstone for a given realization

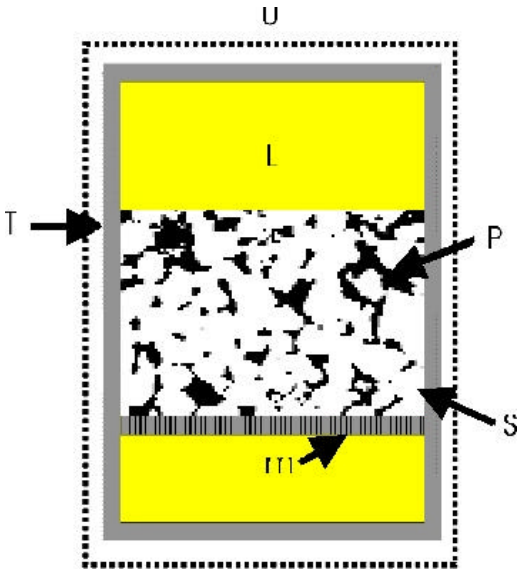

Figure 3: Geometrical problem for fluid invasion into a porous structure M. Solid (S), porous, (P) and free (L), regions are represented and, also, the wall (T). Porous region is M=SUP. The The region of fluids is F=U-TÈS. A semi-permeable membrane (m) is also represented in the figure for preventing bubbling in the free region (L) in the course of the invasion process.

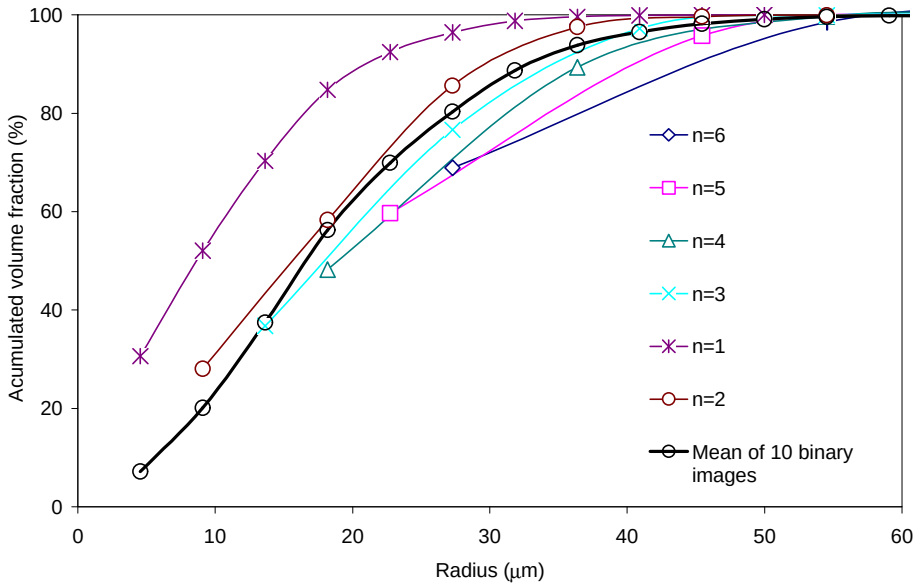

Figure 4: **Comparison between reconstructed representation and original data taken as the mean of 10 binary target petrographic images of a Brazilian sandstone. Reconstruction was performed with a linear size N=200**

Figure 5: Internal Intrusion.

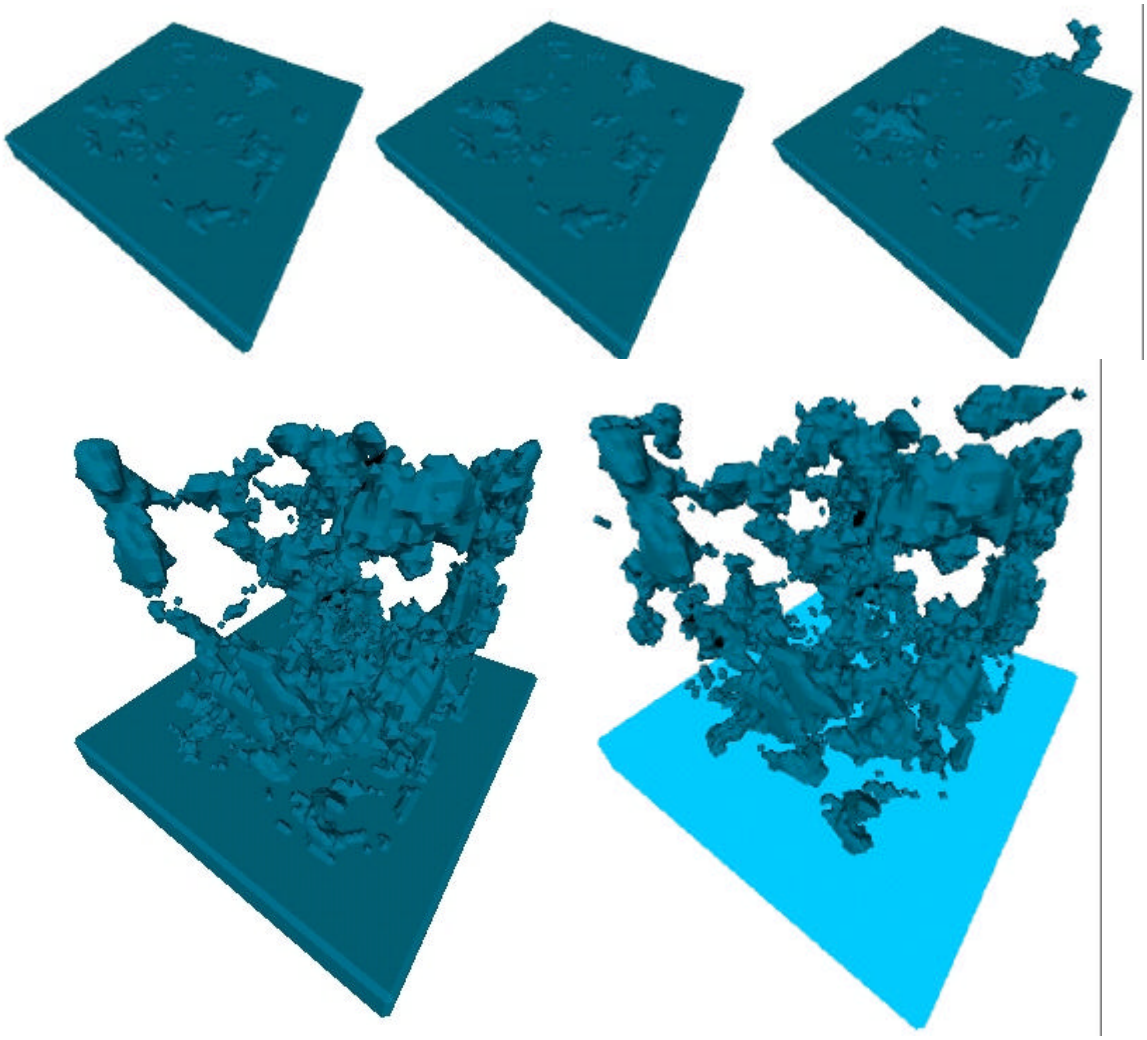

Figure 6: Sequential evolution of mercury 1F intrusion for different pressure steps

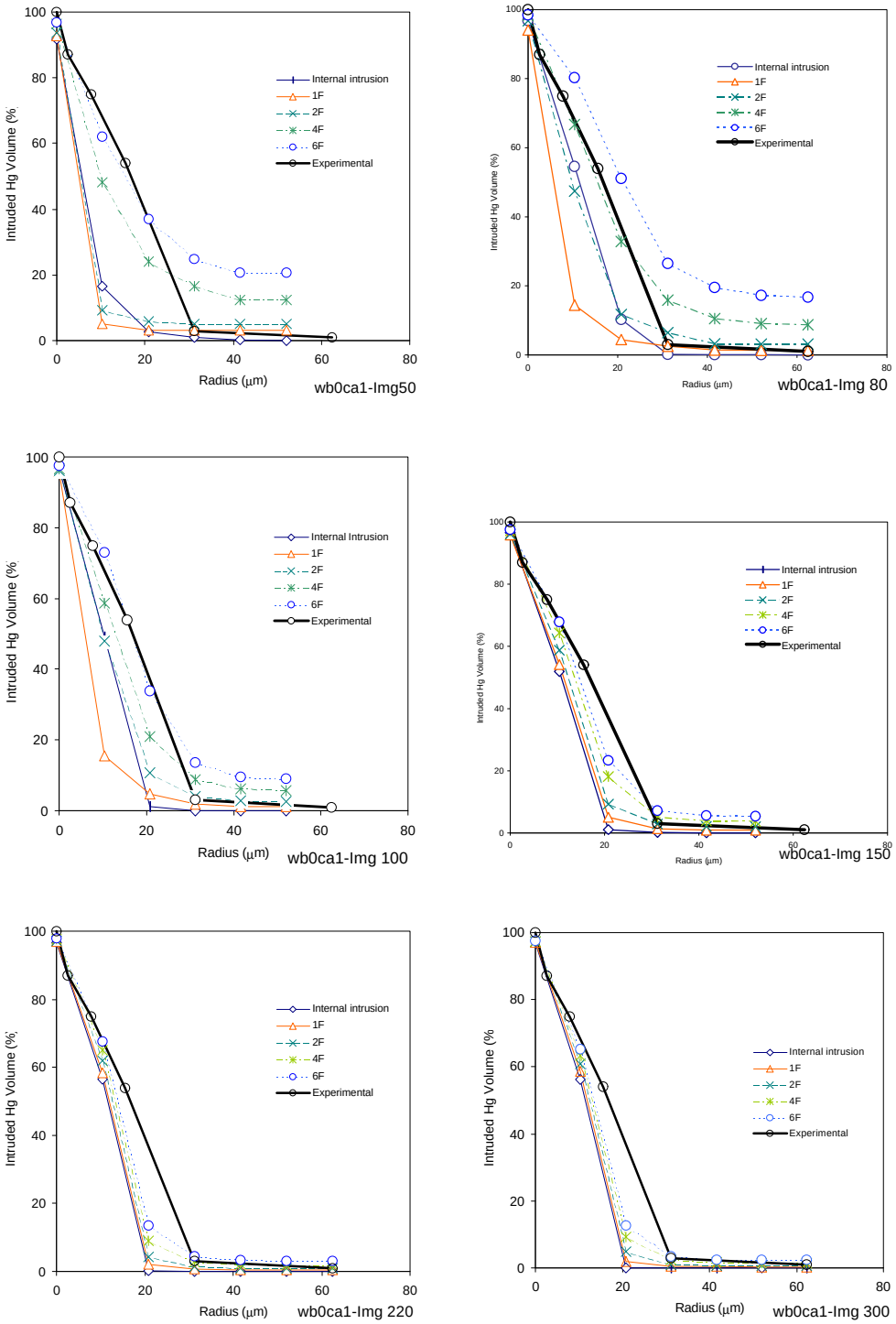

Figure 7: Sequence of simulation results when 3D representation linear size N is increased from 50 to 300. Different curves refer to different intrusion methods: 1F, 2F, 4F, 6F and internal intrusion

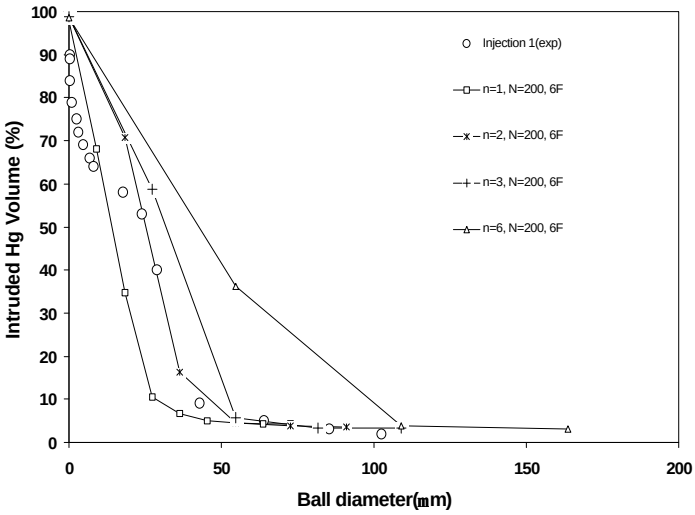

Figure 8: Simulation results for the same Brazilian sandstone shown in Figure 1 (b)

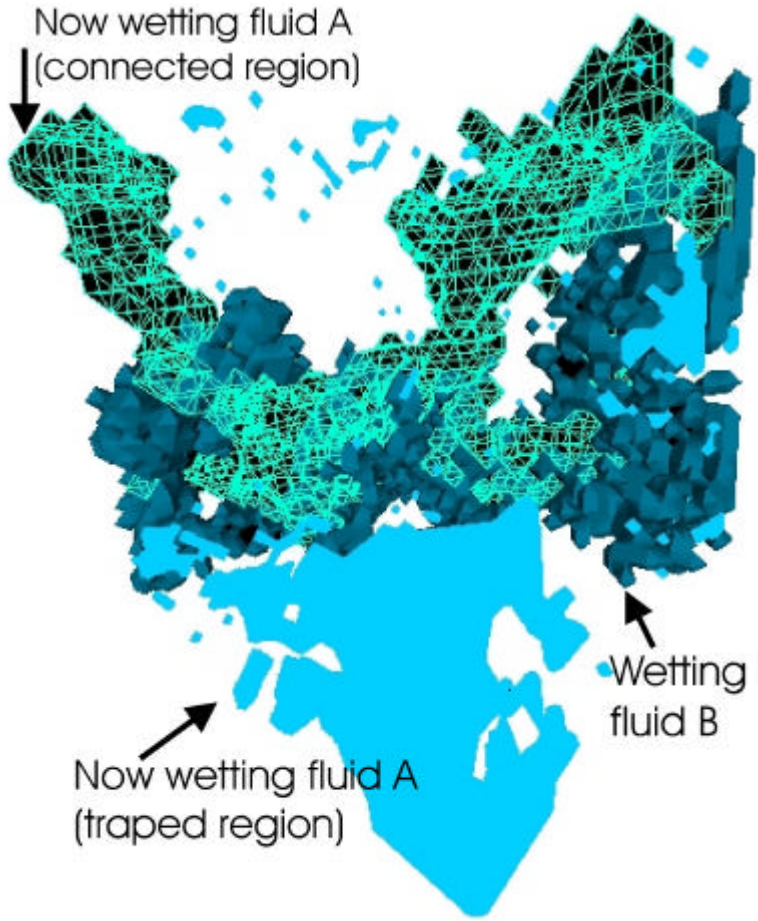

Figure 9: 3D visualization of wetting fluid invasion in to sample sandstone

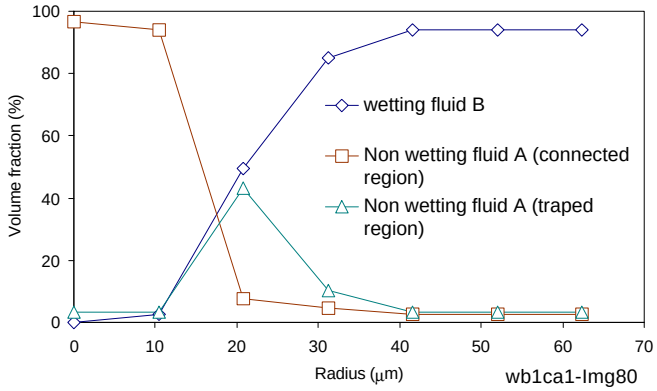

(a)

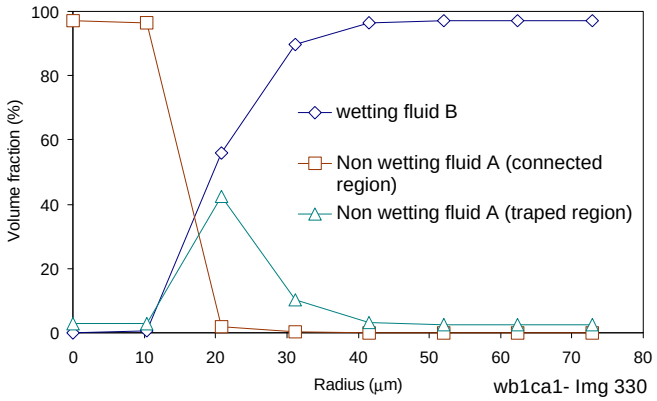

(b)

Figure 10: Wetting fluid B invasion into a Berea500 reconstructed representation initially filled with an ideally compressible non-wetting fluid A (a) 803, n=4, (b) 3303, n=4

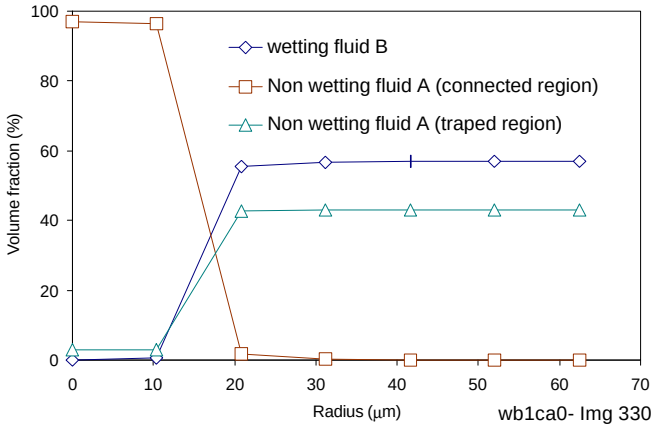

Figure 11: Wetting fluid B invasion into a 3303 Berea500 reconstructed representation initially filled with an ideally non compressible non-wetting fluid A (sampling factor n=4)

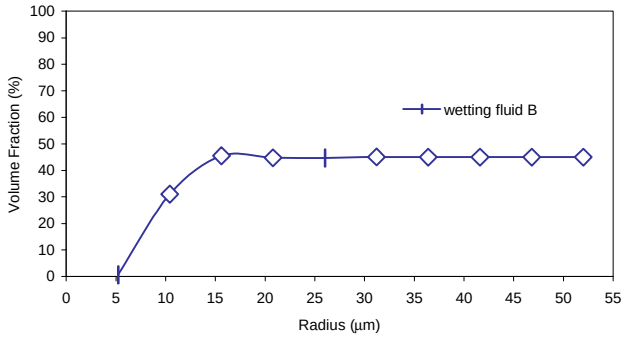

Figure 12**: Wetting fluid B invasion into a Berea 500 reconstructed representation initially filled with an ideally uncompressible non-wettingfluid A (with n=1 as sampling factor)**

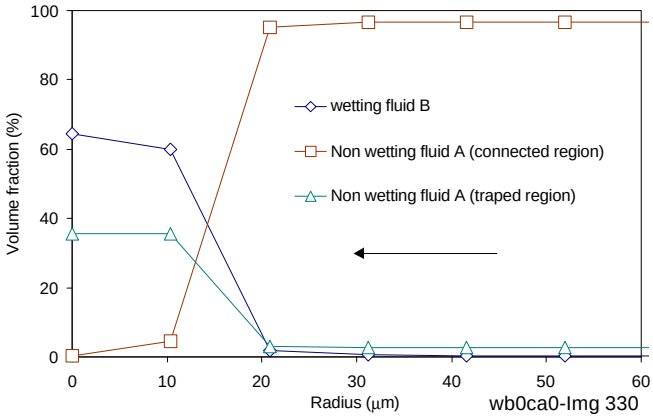

Figure 13: Non-wetting fluid B invasion into a 330 3 Berea500 reconstructed representation initially filled with an ideally non compressible wetting fluid A